

Analysis of a cable-stayed bridge with uncertainties in Young's modulus and load - A fuzzy finite element approach

M. V. Rama Rao[†]

Department of Civil Engineering, Vasavi College of Engineering, Hyderabad-500 031, India

R. Ramesh Reddy[‡]

Department of Civil Engineering, Osmania University College of Engineering, Hyderabad-7, India

(Received June 23, 2006, Accepted April 6, 2007)

Abstract. This paper presents a fuzzy finite element model for the analysis of structures in the presence of multiple uncertainties. A new methodology to evaluate the cumulative effect of multiple uncertainties on structural response is developed in the present work. This is done by modifying Muhanna's approach for handling single uncertainty. Uncertainty in load and material properties is defined by triangular membership functions with equal spread about the crisp value. Structural response is obtained in terms of fuzzy interval displacements and rotations. The results are further post-processed to obtain interval values of bending moment, shear force and axial forces. Membership functions are constructed to depict the uncertainty in structural response. Sensitivity analysis is performed to evaluate the relative sensitivity of displacements and forces to uncertainty in structural parameters. The present work demonstrates the effectiveness of fuzzy finite element model in establishing sharp bounds to the uncertain structural response in the presence of multiple uncertainties.

Keywords: fuzzy finite element model; multiple uncertainties; structural response; sensitivity.

1. Introduction

Analysis and design of structures occupy an important place in the field of Civil Engineering. Modern day structures are usually complex in geometry and are made of a combination of several materials. In order to ensure that structures do not fail during their intended design life period with catastrophic and unpredictable consequences, proper analysis and design are mandatory. Classical finite element analysis is presently the most popular mathematical tool for the analysis of structures. Finite element analysis, being an approximate numerical method, is used to solve a mathematical model in order to make a reasonable prediction of behaviour of structural systems. The parameters used in generating the mathematical model are normally crisp and certain in nature. It is presumed that the structural response of the mathematical model closely corresponds to the behaviour of the

[†] Associate Professor, Ph.D., Corresponding author, E-mail: dr.mvrr@gmail.com

[‡] Professor

actual structure. Any variation in the response of the structure predicted using the mathematical model and the response of the physical structure could be owing to uncertainties involved in material and geometric properties, service loads and boundary conditions. The errors due to these uncertainties can neither be handled nor eliminated by the use of classical finite element analysis. Thus uncertainty needs to be introduced in the engineering analysis and design of structures to enhance the functionality and dependability of the mathematical model of the structure. The uncertainty introduced in the mathematical model of the structure needs to be reflected in the method of analysis and its output as well. This requires the redefinition and extension of the classical finite element model to a fuzzy finite element model, which allows the use of fuzzy interval variables in order to account for uncertainties in parameters.

2. Literature survey

Koyluoglu *et al.* (1995) developed an interval based finite element method to deal with pattern loading and structural uncertainty. In addition, linear programming and triangle inequalities were used for the solution of simultaneous linear interval equations. Köyluoglu and Elishakoff (1998) demonstrated the problem of shear frames with uncertain properties and compared the results obtained by stochastic and interval versions of finite elements.

Rao and Sawyer (1995), Rao and Berke (1997), Rao and Chen Li (1998) have developed different versions of interval-based finite elements to account for uncertainties in engineering problems. But these works were primarily developed to suit narrow intervals and approximate numerical results. Rao and Chen Li (1998) developed a new search-based algorithm to solve a system of linear interval equations. The algorithm performs search operations with an accelerated step size in order to locate the optimal setting of the hull of the solution.

Extensive research helped understanding the behaviour of imprecisely defined systems using fuzzy logic. Use of fuzzy logic to understand and model the behaviour of structural systems is of recent origin. Mullen and Muhanna (1999) developed a fuzzy-based matrix method of structural analysis for the calculation of extreme values of structural response for all possible loading combinations. Concerted efforts were made since then to handle uncertainty in engineering problems realistically by introducing fuzziness in material and geometric properties of structural systems and also in service loads to which the structures are exposed to during their design life period. Muhanna and Mullen (1999) dealt with the formulation by fuzzy-finite elements for solid mechanics problems. The fuzzy approach to treating uncertainties in continuum mechanics is applied to individual instances of load, geometric and material uncertainties thus obtaining sharp enclosure of fuzzy solution in comparison with the exact solution.

A practical approach for analyzing the structures with fuzzy parameters was developed by Akpan *et al.* (2001). The uncertainties in material, loading and structural properties were represented by convex normal fuzzy sets. Vertex solution methodology that was based on α -cut representation was used for the fuzzy analysis. Response surface methodology and combinatorial optimization were used to determine the binary combinations of the fuzzy variables that resulted in fuzzy responses at an α -cut level. These binary combinations of the fuzzy variables were then used to obtain extreme responses to the finite element model.

Muhanna and Mullen (2001) handled uncertainty in mechanics problems by using an interval-based approach. Element-by-element (EBE) technique was employed to obtain a sharp enclosure for

the fuzzy solution by eliminating the sources of overestimation.

A cable-stayed bridge was modelled and analysed using fuzzy-finite element analysis by Rama Rao and Ramesh Reddy (2003). The Centre Canal Bridge at Obourg, Belgium was chosen as an example problem. Uncertainty of live load was introduced by a triangular membership function. Static response of the bridge to the fuzzy interval loading is obtained in terms of fuzzy interval displacements. The results demonstrated the effectiveness of introducing fuzziness in the analysis of cable-stayed bridges.

However the efforts of the previous researchers were confined to the study of the effect of a single uncertainty on the structural behavior. Effect of multiple uncertainties on the structural response was not considered so far. Multiple uncertainties refer to the simultaneous presence and concomitant variation of uncertainties of structural parameters. These uncertainties are considered as fuzzy interval values. Fuzzy finite element analysis has not been hitherto applied to the study of complex structures in order to understand their structural response. There exists no literature, which incorporates multiple uncertainties in the analysis and design of complex structures such as cable-stayed bridges. Thus there is a need to develop fuzzy finite element methodology to evaluate the effect of multiple uncertainties on the structural response. Also, there is a need to study the effect of these uncertainties on the membership functions of the structural response quantities.

In the present work, a new methodology is developed using a fuzzy-finite element model to study the effect of multiple uncertainties on the structural response. The methodology is validated by comparing the results of an example problem with combinatorial solution. The validated methodology is then applied to study the structural response of a cable-stayed bridge with uncertainties in Young's moduli and live load. The sensitivity of structural response to the concomitant variation of load and material uncertainties is also explored.

3. Formulation of linear interval equations-Muhanna's approach

The variational formulation for an interval case of a discrete element-by-element structural model is given as (Muhanna and Mullen 2001)

$$\Pi = \frac{1}{2} \{U\}^T [K] \{U\} - \{U\}^T \{P\} + \{\lambda\}^T \{[\tilde{C}] \{U\} - \{V\}\} \quad (1)$$

where Π , $[K]$, $[\tilde{C}]$, $\{U\}$, $\{P\}$ and $\{\lambda\}$ are potential energy, stiffness matrix, constraint matrix, displacement vector and load vector and vector of Lagrange multipliers respectively. In this model, elements are kept separate throughout the course of the solution and constraints are imposed to ensure the compatibility of displacement of coincident nodes. Constraints are imposed on coincident nodes as

$$[\tilde{C}] \{U\} = \{0\} \quad (2)$$

Using Rayleigh-Ritz approach and invoking the stationarity of Π leads to

$$\{U\} = [\tilde{R}]^{-1} [D]^{-1} \{ \{P\} - [\tilde{C}]^T \{\lambda\} \} \quad (3)$$

where

$$[K] = [D][\tilde{S}] \quad (4)$$

and

$$[\tilde{R}] = [\tilde{S}] + [\tilde{C}]^T [\tilde{C}] \quad (5)$$

Here $[\tilde{S}]$ is a deterministic singular matrix of size $n \times n$ and $[D]$ is a diagonal matrix of size $n \times n$ containing interval terms corresponding to uncertain Young's modulus. Eq. (3) was solved by Muhanna (Muhanna and Mullen 2001) by approximating the vector of internal forces $\{\lambda\}$ by its mid-point (crisp) vector $\{\lambda_c\}$ to solve the equations when the load vector $\{P\}$ is crisp and Young's modulus is uncertain.

3.1 Avoiding overestimation – present approach

Attempts by the authors to apply Muhanna's approach in the presence of load and material uncertainties resulted in an overestimated solution. It is found that the overestimation is due to

- a) coupling of elements of the interval load vector at the elemental level itself due to contribution of various interval loads simultaneously acting on each element.
- b) approximating of the interval vector of internal forces $\{\lambda\}$ by its mid-point (crisp) vector $\{\lambda_c\}$. Overestimation of displacement vector is eliminated in the present work by
- a) keeping the contribution of the loads to the overall solution separate throughout the solution process in order to eliminate overestimation due to coupling of load vector.
- b) developing a new approximation to the vector of internal forces.

4. Handling multiple uncertainties – present study

Using extension principle, Eqs. (2) and (3) can be rewritten at given levels of material uncertainty α and load uncertainty β ($0 \leq \alpha, \beta \leq 1$) as

$$[\tilde{C}]\{U_{\alpha\beta}\} = \{0\} \quad (6)$$

$$\{U_{\alpha\beta}\} = [\tilde{R}]^{-1}[D_\alpha]^{-1}\{\{P_\beta\} - [\tilde{C}]^T\{\lambda_{\alpha\beta}\}\} \quad (7)$$

where $[K_\alpha]$ is interval stiffness matrix and $[D_\alpha]$ is an diagonal interval matrix at a specified level of material uncertainty α , $\{P_\beta\}$ is interval load vector at a specified level of load uncertainty β . Further, $\{\lambda_{\alpha\beta}\}$ and $\{U_{\alpha\beta}\}$ correspond to the interval internal force vector and interval displacement vector respectively at a specified levels of material and load uncertainties α and β . It may be here noted that $[K_\alpha]$ and $[D_\alpha]$ are functions of α alone, $\{P_\beta\}$ is a function of β alone, while $\{\lambda_{\alpha\beta}\}$ and $\{U_{\alpha\beta}\}$ are functions are both α and β .

The interval stiffness matrix $[K_\alpha]$ is a symmetric indefinite square matrix owing to the de-assembled state of elements in the EBE model (Muhanna and Mullen 2001). All the elements of the stiffness matrix have the Young's modulus as the multiplier. Therefore, stiffness uncertainty for an element is equal to the material uncertainty α (of the Young's modulus). The size of $[K_\alpha]$ is $n \times n$ where n is the product of number of degrees of freedom per each element and total number of elements in the structure. The vector $\{\lambda_{\alpha\beta}\}$ represents the internal forces that are exposed because elements in the EBE model are kept separate till the end. If the interval vector $\{\lambda_{\alpha\beta}\}$ can be determined exactly, then

the solution of Eq. (7) represents the exact hull of interval system of equations

$$[K]\{U\} = \{P\} \quad (8)$$

In the case of statically indeterminate structures, $\{\lambda_{\alpha\beta}\}$ depends on uncertain structural stiffness (at a level α) addition to uncertain load (at a level β) and boundary conditions (crisp). Therefore evaluation of the exact value of $\{\lambda_{\alpha\beta}\}$ is uncertain.

Following section 3.1, the contribution of each the loads acting on the structure to the overall solution is kept separate throughout the solution process. Thus the vector of internal forces $\{\lambda_{\alpha\beta}\}$ due to each of the loads acting on the structure is approximated as

$$\{\lambda_{\alpha\beta}\} \approx [\beta_1, \beta_u]\{\lambda_{cc}\} \quad (9)$$

The above approximation is validated in the section 5.1.

Substituting Eq. (9) in Eq. (7) leads to

$$[D_\alpha][\tilde{R}]\{U_{\alpha\beta}\} = \{\{P_\beta\} - [\beta_1, \beta_u][\tilde{C}]^T\{\lambda_{cc}\}\} \quad (10)$$

Eq. (10) can be expressed as

$$\{U_{\alpha\beta}\} = [\tilde{R}]^{-1}[M]\{\delta_\alpha\} \quad (11)$$

where $[M]$ is a matrix of size $n \times m$ where m is the number of elements and $\{\delta_\alpha\}$ is an interval vector of size $m \times 1$ containing interval Young's modulus of m elements taken from the diagonal entries of $[D_\alpha]$.

In order to solve Eq (11), it is necessary to compute the value of the mid-point internal force vector $\{\lambda_{cc}\}$. This is done by analysing the assembled finite element model of the structure with crisp value of structural stiffness subjected to fuzzy interval loading with uncertainty β . Eq. (11) represents a set of interval matrix equations. Solution of these equations using the inclusion theory results in an optimal enclosure known as the hull of the solution (Fig. 1). Making use of Jansson's algorithm (Jansson 1991), the lower bound vector $\{x\}$ and the upper bound vector $\{y\}$ enclosing the hull of the solution are obtained. The solution vector $[U_{\alpha\beta}]$ is taken as the average of $\{x\}$ and $\{y\}$. The vector of internal forces for an element is obtained as

$$\{\lambda_{\alpha\beta}\}_{md \times 1}^{(e)} = [\beta_1, \beta_u][\mathbf{K}_\alpha]_{md \times md}^{(e)}[T]_{md \times md}^{(e)}[L]_{md \times n}[\tilde{R}]^{-1}[\mathbf{M}]\{\delta\}_\alpha - \{\mathbf{P}_\beta\}_{md \times 1}^{(e)} \quad (12)$$

where $[L]_{md \times n}$ is a Boolean connectivity matrix containing 0^s and 1^s, $[T^{(e)}]$ is the rotation transformation matrix for the element and md is the number of degrees of freedom for the element.

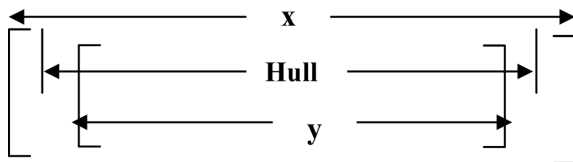


Fig. 1 Bounds on hull solution

5. Validation of the present approach

A two-bay two-floor frame as shown in Fig. 2 is taken up to validate the present approach. The properties of the frame are listed in Table 1. The frame is subjected to uncertain loads w_1 , w_2 , w_3 and w_4 acting on the beams 7, 8, 9 and 10. All the uncertain parameters are assumed to vary independently. The results for displacements of nodes 4 and 9 of the two-floor two-bay frame are given in Table 2. Combinatorial solution is obtained by introducing all possible combinations of the bounds of the interval parameters into analysis and establishing the lower and upper bounds of the structural response. The present approach leads to sharp bounds of the exact solution of displacements with errors within a range of 0.002% to 0.162%. The corresponding errors for forces and moments lie within the range of 0.68% to 0.944%. It is observed that the results obtained yielded sharp bounds to the combinatorial solution, thus validating the present method.

Table 1 Properties of two bay – two floor frame

Columns	Area of Cross section	0.4 m^2	Moment of Inertia	0.036 m^4
Beams	Area of Cross section	0.6 m^2	Moment of Inertia	0.08 m^4
Young's Modulus = [199,201] GPa		$w_1 = w_2 = [24, 26] \text{ kN/m}$	$w_3 = w_4 = [48, 52] \text{ kN/m}$	

Table 2 Two bay two floor Frame – Displacements and forces

Response	Comb	Present	Error (Lower bound)	Error (Upper bound)
$V_4 \times 10^{-6} (\text{m})$	$[-6.7640, -6.1548]$	$[-6.7660, -6.1530]$	0.029%	0.029%
$V_9 \times 10^{-6} (\text{m})$	$[-13.0697, -11.9207]$	$[-13.070, -11.920]$	0.002%	0.006%
$\theta_9 \times 10^{-6} (\text{rad})$	$[5.6331, 6.2691]$	$[5.624, 6.279]$	0.162%	0.16%
$N_1 (\text{kN})$	$[-149.676, -137.3503]$	$[-151.090, -136.066]$	0.944%	0.935%
$V_1 (\text{kN})$	$[5.2608, 5.8790]$	$[5.224, 5.919]$	0.699%	0.68%
$M_1 (\text{kNm})$	$[-14.1977, -12.5250]$	$[-14.297, -12.431]$	0.699%	0.75%

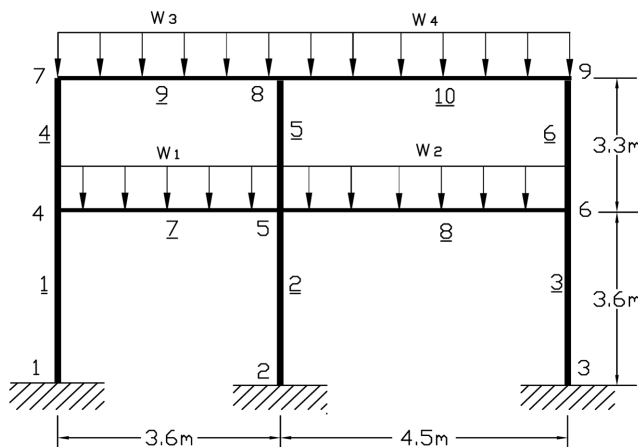


Fig. 2 Two-bay two-floor frame

Table 3 Two bay two storey truss with load on beam 10 alone – Forces and moments at node 5

Description	$\{\lambda_{cc}\}$	$[\beta_1, \beta_u]\{\lambda_{cc}\}$	$\{\lambda_{\alpha\beta}\}$	Relative error	
				Lower bound	Upper bound
N_5 (kN)	-119.451	[-124.22, -114.67]	[-125.507, -113.394]	1.025%	1.125%
V_5 (kN)	14.1215	[13.556, 14.686]	[13.385, 14.858]	1.277%	1.158%
M_5 (kNm)	-32.944	[-34.262, -31.626]	[-34.620, -31.268]	1.034%	1.145%

5.1 Validation of the approximation of vector of internal forces $\{\lambda_{\alpha\beta}\}$

The above two-bay two-floor frame is now subjected to uniformly distributed load w_4 alone. The uncertain load and Young's modulus correspond to $[\beta_1, \beta_u] = [0.96, 1.04]$ and $[\alpha_1, \alpha_u] = [0.995, 1.005]$. The axial force N_5 , shear force V_5 and bending moment M_5 at node 5 are presented in Table 3. In this table, $\{\lambda_{cc}\}$ refers to crisp values of forces and moments while $\{\lambda_{\alpha\beta}\}$ refers to the interval forces and moments. Relative error computed between the lower and upper bounds of $\{\lambda_{\alpha\beta}\}$ and $[\beta_1, \beta_u]\{\lambda_{cc}\}$ is presented in the last column. It is observed at the percentage of relative error is limited to the range of 1.025% to 1.145%. This validates the approximation made in Eq. (9).

6. Case study

The case study considered is a cable-stayed bridge with fan configuration of cable-stays, shown in Fig. 3. This problem is adopted from the configuration of *Canal du Centre Bridge* at Obourg, Belgium (Walther 1988). The properties of the bridge are mentioned in Table 4. The bridge is symmetric about the longitudinal axis. Owing to the symmetry of the bridge deck about the longitudinal axis of the bridge, only one half of the bridge along with a single plane of cables is used for analysis. The structural elements belonging to bridge deck and the pylon are idealized as plane frame elements while cables are modelled as bar elements. The cable-stayed bridge described above is subjected to the action of a uniformly distributed live load. Membership functions of uncertainties α and β of Young's modulus and live load adopted for the bridge are indicated in Fig. 4 and Fig. 5.

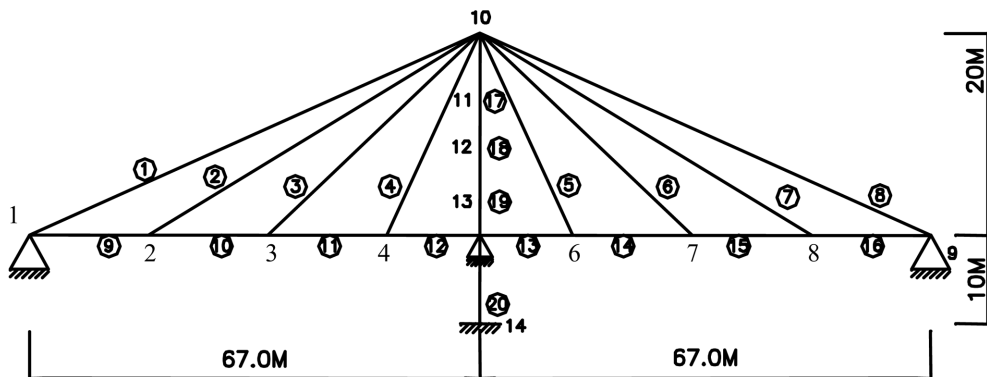


Fig. 3 Cable stayed bridge

Table 4 Properties of cable stayed bridge

Description		Pedestrian foot bridge across <i>Canal du Centre</i> , Belgium of span $2 \times 67.0 = 134.0$ m						
Concrete Deck Slab		Double T Section made of Pre-cast PSC						
Overall width		1.8 m	Depth	0.6 m	Flange thickness	0.20 m	Web thickness	0.3 m
Pylon	Double armed Rectangular Pylon, each arm 0.60×0.80 m with height 20 m above deck (30 m total height)							
Cables	Stranded cables each with 37 strands of $12.7 \text{ mm } \phi$			Young's Modulus	30 GPa (Concrete), 200 GPa(Steel)			
Live Load	4.0 kN/m ²		Material uncertainty		$\pm 5\%$	Load uncertainty	$\pm 10\%$ about mean	

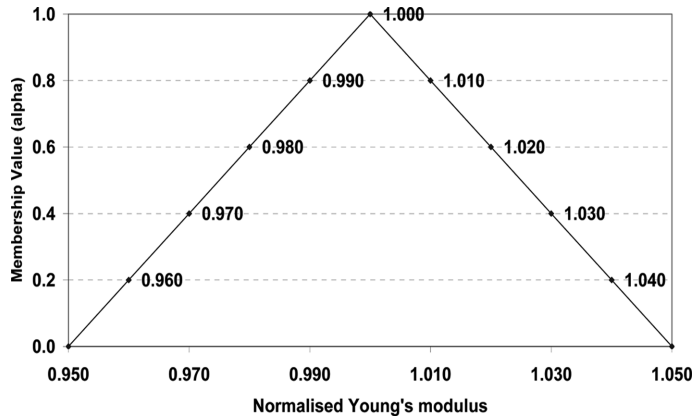


Fig. 4 Membership function for Uncertainty of Young's modulus

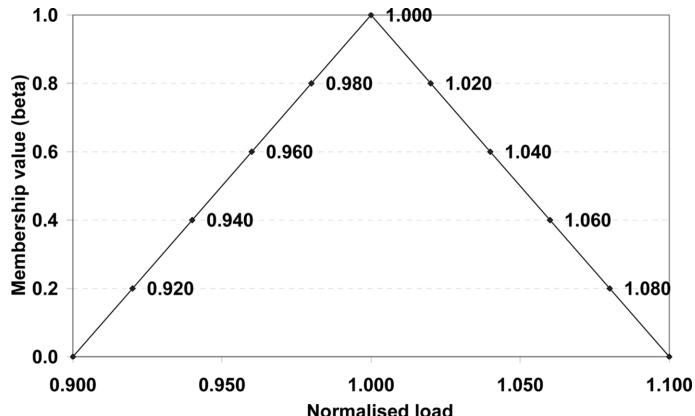


Fig. 5 Membership function for load uncertainty

7. Results and discussion

Table 5, Table 6 and Table 7 show the concomitant variation of horizontal displacement at node 2, vertical displacement at node 3 and rotation at node 4 respectively for various combinations of α and β . Table 8 represents the concomitant variation of bending moment in deck at node 4 whereas Table

9 represents the variation of axial force in deck at node 12. Table 10 shows the concomitant variation of shear force in deck at node 3. Table 11 represents the variation of axial force in cable 3. In all the above tables, the variation of interval-width of structural response is found to be less with variation of material uncertainty in comparison with to live load uncertainty. This is because of the larger uncertainty associated with load ($\pm 10\%$) compared to the uncertainty of Young's modulus ($\pm 5\%$).

Table 5 Concomitant Variation of Horizontal displacement of node 2 ($\times 10^{-4}$ m) w.r.t α and β

$\alpha \downarrow \beta \rightarrow$	1.0	0.8	0.6	0.4	0.2	0.0
1.0	[3.275,3.275]	[3.169,3.382]	[3.063,3.488]	[2.956,3.595]	[2.850,3.701]	[2.743,3.808]
0.8	[3.198,3.353]	[3.095,3.458]	[2.989,3.565]	[2.883,3.672]	[2.777,3.779]	[2.671,3.886]
0.6	[3.122,3.432]	[3.021,3.535]	[2.915,3.643]	[2.810,3.750]	[2.704,3.858]	[2.599,3.965]
0.4	[3.046,3.511]	[2.948,3.613]	[2.843,3.721]	[2.738,3.829]	[2.632,3.937]	[2.527,4.045]
0.2	[2.970,3.591]	[2.875,3.691]	[2.770,3.800]	[2.666,3.909]	[2.561,4.018]	[2.456,4.126]
0.0	[2.896,3.672]	[2.803,3.770]	[2.698,3.880]	[2.594,3.989]	[2.490,4.099]	[2.437,5.337]

Table 6 Concomitant Variation of Vertical displacement of node 3 ($\times 10^{-2}$ m) w.r.t α and β

$\alpha \downarrow \beta \rightarrow$	1.0	0.8	0.6	0.4	0.2	0.0
1.0	[-1.474,-1.474]	[-1.604,-1.344]	[-1.734,-1.214]	[-1.864,-1.084]	[-1.994,-0.953]	[-2.124,-0.823]
0.8	[-1.566,-1.382]	[-1.696,-1.253]	[-1.827,-1.123]	[-1.957,-0.993]	[-2.088,-0.863]	[-2.218,-0.733]
0.6	[-1.658,-1.291]	[-1.789,-1.162]	[-1.920,-1.032]	[-2.051,-0.902]	[-2.182,-0.773]	[-2.313,-0.644]
0.4	[-1.750,-1.200]	[-1.882,-1.071]	[-2.013,-0.942]	[-2.145,-0.812]	[-2.276,-0.683]	[-2.408,-0.554]
0.2	[-1.843,-1.109]	[-1.975,-0.980]	[-2.107,-0.853]	[-2.239,-0.722]	[-2.372,-0.593]	[-2.504,-0.465]
0.0	[-1.937,-1.018]	[-2.069,-0.889]	[-2.202,-0.761]	[-2.335,-0.632]	[-2.467,-0.504]	[-2.600,-0.375]

Table 7 Concomitant Variation of Rotation at node 4 ($\times 10^{-3}$ radians) w.r.t α and β

$\alpha \downarrow \beta \rightarrow$	1.0	0.8	0.6	0.4	0.2	0.0
1.0	[0.381,0.381]	[0.306,0.456]	[0.231,0.530]	[0.156,0.605]	[0.081,0.680]	[0.006,0.754]
0.8	[0.328,0.434]	[0.253,0.509]	[0.178,0.584]	[0.103,0.659]	[0.028,0.734]	[-0.045,0.809]
0.6	[0.275,0.487]	[0.199,0.563]	[0.125,0.638]	[0.051,0.713]	[-0.023,0.788]	[-0.098,0.863]
0.4	[0.221,0.541]	[0.146,0.616]	[0.072,0.692]	[-0.002,0.767]	[-0.076,0.842]	[-0.151,0.918]
0.2	[0.168,0.595]	[0.098,0.670]	[0.019,0.746]	[-0.054,0.821]	[-0.129,0.897]	[-0.203,0.972]
0.0	[0.115,0.648]	[0.041,0.724]	[-0.033,0.800]	[-0.107,0.876]	[-0.182,0.951]	[-0.256,1.028]

Table 8 Concomitant Variation of Bending Moment (kNm) in deck at node 4 w.r.t α and β

$\alpha \downarrow \beta \rightarrow$	1.0	0.8	0.6	0.4	0.2	0.0
1.0	[-83.2,-83.2]	[-85.7,-80.5]	[-88.3,-77.9]	[-90.9,-75.3]	[-93.5,-72.7]	[-96.2,-70.1]
0.8	[-86.1,-80.2]	[-88.7,-77.6]	[-91.4,-75.0]	[-94.0,-72.4]	[-96.6,-69.8]	[-99.3,-67.2]
0.6	[-89.2,-77.3]	[-91.8,-74.6]	[-94.4,-72.1]	[-97.1,-69.5]	[-99.7,-67.0]	[-102.4,-64.4]
0.4	[-92.2,-74.3]	[-94.8,-71.7]	[-97.5,-69.2]	[-100.2,-66.7]	[-102.9,-64.1]	[-105.6,-61.6]
0.2	[-95.3,-71.4]	[-97.9,-68.9]	[-100.6,-66.3]	[-103.4,-63.8]	[-106.1,-61.3]	[-108.8,-58.7]
0.0	[-98.4,-68.5]	[-101.1,-66.0]	[-103.8,-63.5]	[-106.5,-61.0]	[-109.3,-58.4]	[-112.0,-55.9]

Table 9 Concomitant Variation of Axial Force in deck in element 12 (kN) w.r.t α and β

$\alpha \downarrow \beta \rightarrow$	1.0	0.8	0.6	0.4	0.2	0.0
1.0	[-128.1,-128.1] [-130.7,-125.5] [-133.2,-123.0] [-135.8,-120.4] [-138.3,-117.8] [-140.9,-115.3]					
0.8	[-132.1,-124.2] [-134.7,-121.7] [-137.4,-119.2] [-140.0,-116.7] [-142.7,-114.2] [-145.3,-111.8]					
0.6	[-136.2,-120.4] [-138.9,-118.0] [-141.7,-115.6] [-144.4,-113.1] [-147.1,-110.7] [-149.9,-108.3]					
0.4	[-140.5,-116.7] [-143.3,-114.3] [-146.1,-112.0] [-148.9,-109.7] [-151.7,-107.3] [-154.5,-105.0]					
0.2	[-144.8,-113.0] [-147.7,-110.8] [-150.6,-108.5] [-153.5,-106.3] [-156.4,-104.0] [-159.3,-101.7]					
0.0	[-149.3,-109.5] [-152.3,-107.3] [-155.3,-105.1] [-158.3,-102.9] [-161.3,-100.7] [-164.2,-98.5]					

Table 10 Concomitant Variation of Shear Force in deck at node 3 (kN) w.r.t α and β

$\alpha \downarrow \beta \rightarrow$	1.0	0.8	0.6	0.4	0.2	0.0
1.0	[31.64, 31.64]	[30.86,32.41]	[30.09,33.17]	[29.32,33.94]	[28.55,34.71]	[27.78,35.49]
0.8	[31.02, 32.26]	[30.25,33.04]	[29.49,33.82]	[28.73,34.60]	[27.96,35.37]	[27.20,36.15]
0.6	[30.41, 32.89]	[29.65,33.68]	[28.90,34.47]	[28.14,35.26]	[27.39,36.05]	[26.63,36.83]
0.4	[29.81, 33.54]	[29.06,34.34]	[28.31,35.13]	[27.56,35.93]	[26.81,36.73]	[26.07,37.52]
0.2	[29.21, 34.19]	[28.47,35.00]	[27.73,35.81]	[26.99,36.61]	[26.25,37.42]	[25.51,38.23]
0.0	[28.62, 34.86]	[27.89,35.68]	[27.15,36.49]	[26.42,37.31]	[25.69,38.12]	[24.96,38.94]

Table 11 Concomitant Variation of Axial Force (kN) in cable 3 w.r.t α and β

$\alpha \downarrow \beta \rightarrow$	1.0	0.8	0.6	0.4	0.2	0.0
1.0	[129.62,129.62]	[126.48,132.75]	[123.34,135.89]	[120.20,139.03]	[117.06,142.17]	[113.92,145.31]
0.8	[124.80,134.53]	[121.72,137.73]	[118.65,140.94]	[115.57,144.15]	[112.50,147.35]	[109.42,150.56]
0.6	[120.06,139.54]	[117.05,142.81]	[114.03,146.09]	[111.02,149.36]	[108.01,152.64]	[105.00,155.91]
0.4	[115.41,144.65]	[112.45,148.00]	[109.50,151.35]	[106.55,154.69]	[103.59,158.04]	[100.64,161.39]
0.2	[110.83,149.88]	[107.93,153.30]	[105.03,156.72]	[102.14,160.14]	[99.24,163.56]	[96.34,166.99]
0.0	[106.32,155.22]	[103.47,158.71]	[100.63,162.21]	[97.79,165.72]	[94.95,169.22]	[92.11,172.72]

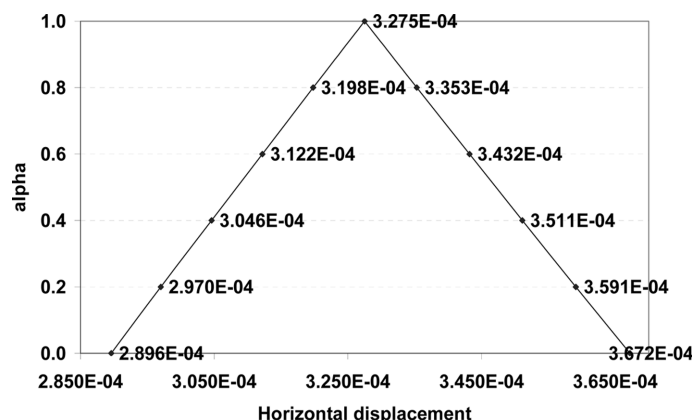


Fig. 6 Membership Function for horizontal displacement at node 2 at beta = 1.0

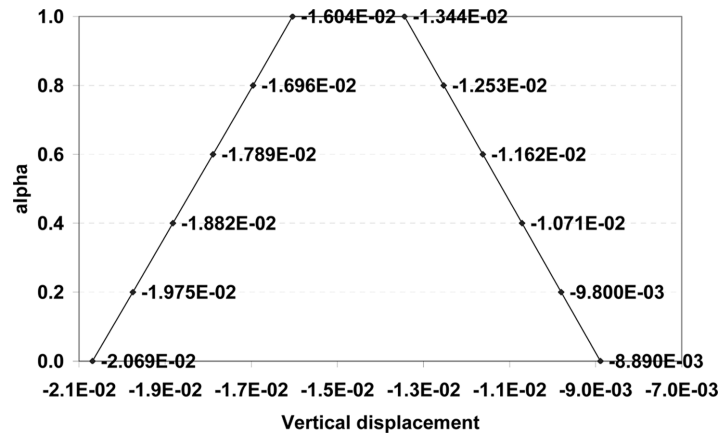


Fig. 7 Membership function for vertical displacement at node 3 at beta = 0.8

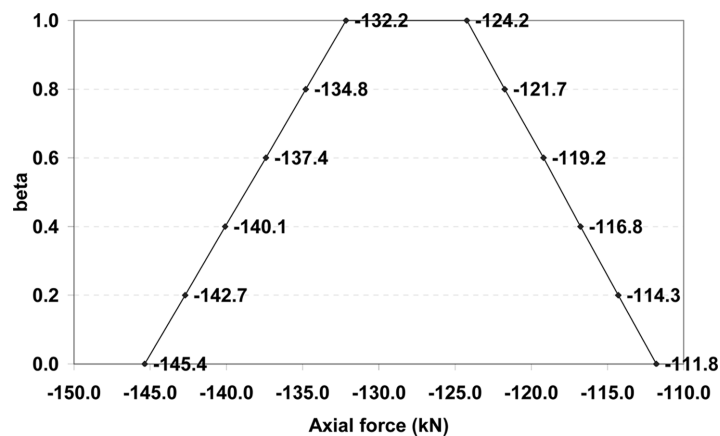


Fig. 8 Membership function for Axial force in element 12 at alpha = 0.8

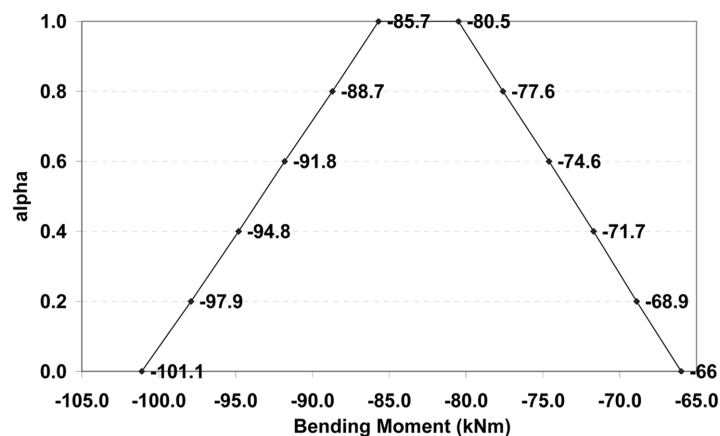


Fig. 9 Membership function for Bending moment at node 4 at beta = 0.8

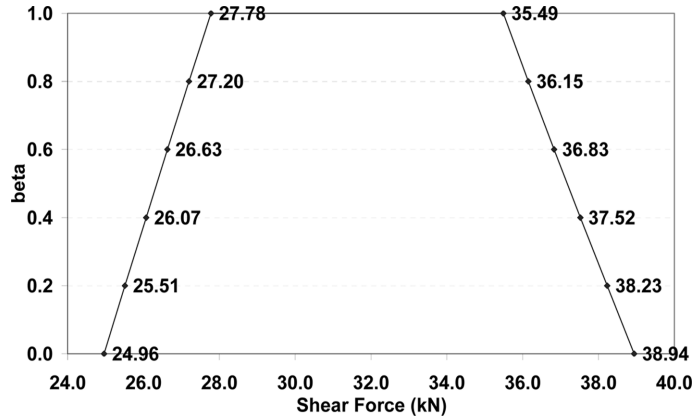


Fig. 10 Membership function for Shear Force at node 3 at beta = 0.8

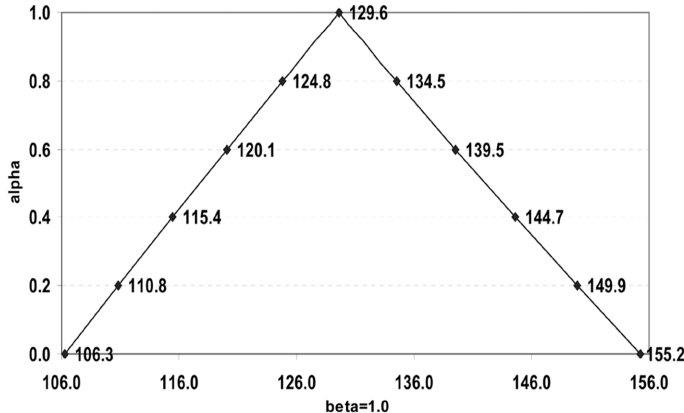


Fig. 11 Membership function for Axial Force (kN) in Cable 3 at beta = 1.0

Fig. 6 represents the membership function for horizontal displacement at node 2 at $\beta=1.0$. Fig. 7 represents the membership function for vertical displacement at node 3 at $\beta=0.8$. Fig. 8 represents the membership function for axial force in deck in element 12 at $\alpha=0.8$. Fig. 9 represents the membership function for bending moment in deck at node 4 at $\beta=0.8$. Fig. 10 represents the membership function for shear force in deck at node 3 at $\beta=0.8$. Fig. 11 represents the membership function for axial force (kN) in cable 3 at $\beta=1.0$. It is observed in all the cases that the membership functions are triangular in the presence of a single uncertainty and are trapezoidal in the presence of multiple uncertainties.

8. Sensitivity analysis

Sensitivity analysis aims at analyzing the relative variation of structural response to a given variation of structural parameters. Percentage variation about the mean value is computed after normalisation of the intervals. An interval $[a, b]$ can be normalised by dividing its lower and upper bounds a and b by the mid-point $\mu = 0.5 * (a + b)$. Thus a Young's modulus [199,201] GPa can be normalised as [0.995,1.005], the variation about the mean being $\pm 0.5\%$. In general, a normalised

interval $[1 - \varepsilon_1, 1 + \varepsilon_2]$ indicates that lower bound and upper bound variations of the given interval about its nominal (mean) value are ε_1 and ε_2 respectively.

Fig. 12 depicts the relative sensitivity of horizontal and vertical displacements and rotation of the deck under the action of live load at $\beta = 1.0$ with respect to percentage variation of Young's modulus about its mean value. The slopes of these plots are 3.05, 5.69 and 6.22 respectively. Similarly, Fig. 13 depicts the relative sensitivity of these displacements at $\alpha = 1.0$ with respect to percentage variation of live load about its mean value. The slopes of these plots are 2.232, 4.377 and 4.422 respectively. It is observed from Fig. 12 and Fig. 13 that the greatest sensitivity (steeper slope) to the variation of the Young's modulus (from the mean) is exhibited by vertical displacement while the lowest sensitivity is exhibited by horizontal displacement. Further, it is observed that the displacements are more sensitive to the variation of Young's modulus in comparison to the variation of the load. A study of sensitivity of displacements other nodes also yielded similar results.

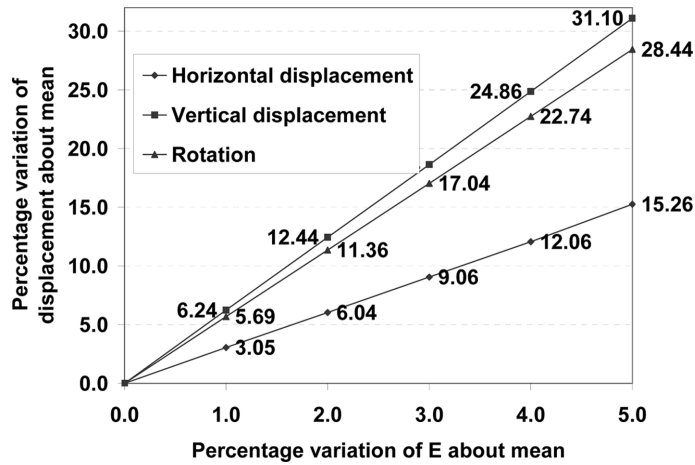


Fig. 12 Sensitivity of displacements at node 3 at beta = 1.0

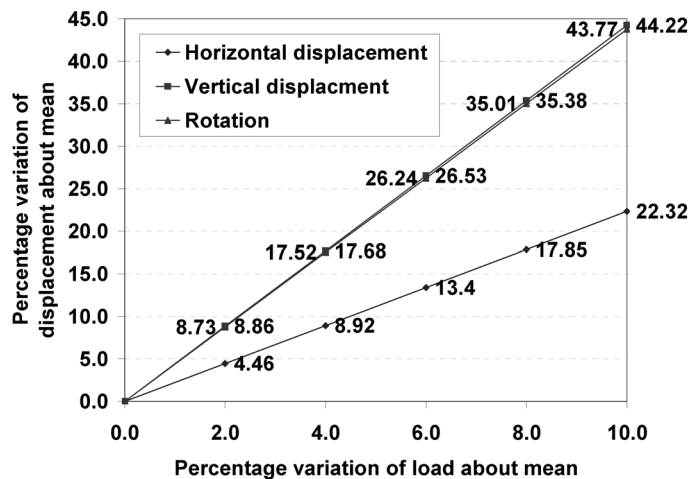


Fig. 13 Sensitivity of displacements at alpha = 1.0

9. Conclusions

In this paper, the interval-based approach proposed by Muhanna and Mullen has been modified to take into account the multiple uncertainties in Young's modulus and live load concomitantly. A sharp enclosure to the solution vector is obtained by uncoupling of load vector by keeping the load contributions separate throughout the solution process. A new approximation to the vector of internal forces is found to yield a sharp solution. The proposed method is illustrated by applying it to the problem of a cable-stayed bridge. Structural response is tabulated and is found to vary for various combinations of load and material uncertainties. Membership functions are found to be triangular in the presence of a single uncertainty and trapezoidal in the presence of multiple uncertainties. The effectiveness of the new methodology to evaluate the structural response of a cable-stayed bridge in the presence of multiple uncertainties is demonstrated. Sensitivity analysis is found to be a useful tool to evaluate the relative sensitivity of structural response in the presence of multiple uncertainties.

References

- Akpan, U.O., Koko, T.S., Orisamolu, I.R. and Gallant, B.K. (2001), "Practical fuzzy finite element analysis of structures", *Finite Elem. Anal. Des.*, **38**, 93-111. (Elsevier Publishing).
- Jansson, C. (1991), "Interval linear systems with symmetric matrices, skew-symmetric matrices, and dependencies in the right hand side", *Computing*, **46**, 265-274.
- Köyluoglu, H.U., Cakmak, A.S. and Nielsen, S.R.K. (1995), "Interval algebra to deal with pattern loading and structural uncertainty", *J. Eng. Mech.*, ASCE, **121**(11), 1149-1157.
- Köyluoglu, H.U. and Elishakoff, I. (1998), "A comparison of stochastic and interval finite elements applied to shear frames with uncertain stiffness properties", *Comput. Struct.*, **67**(1-3), 91-98.
- Muhanna, R.L. and Mullen, R.L. (1999), "Formulation of fuzzy finite element methods for solid mechanics problems", *Comput. Aided Civil Infrastructure Eng.*, **14**, 107-117.
- Muhanna, R.L. and Mullen, R.L. (2001), "Uncertainty in mechanics problems – interval based approach", *J. Eng. Mech.*, ASCE, **127**(6), 557-566.
- Mullen, R.L. and Muhanna, R.L. (1999), "Bounds of structural response for all possible loading combinations", *J. Struct. Eng.*, ASCE, **125**(1), 98-106.
- Rama Rao, M.V. and Ramesh Reddy, R. (2003), "Fuzzy finite element analysis of a cable- stayed bridge", *8th Int. Conf. on Innovations in Planning, Design and Construction Techniques in Bridge Engineering*, Hyderabad, India.
- Rao, S.S. and Sawyer, P. (1995), "Fuzzy finite element approach for analysis of imprecisely defined systems", *AIAA J.*, **33**(12), 2364-2370.
- Rao, S.S. and Berke, L. (1997), "Analysis of uncertain structural systems using interval analysis", *AIAA J.*, **35**(4), 727-735.
- Rao, S.S. and Li Chen (1998), "Numerical solution of fuzzy linear equations in engineering analysis", *Int. J. Numer. Meth. Eng.*, **43**, 391-408.
- Walther, Rene (1988), "Cable Stayed Bridges", Thomas Telford, London.